

# Evaluating water stress in irrigated olives: correlation of soil water status, tree water status, and thermal imagery

Alon Ben-Gal · Nurit Agam · Victor Alchanatis ·  
Yafit Cohen · Uri Yermiyahu · Isaac Zipori ·  
Eugene Presnov · Michael Sprintsin · Arnon Dag

Received: 5 October 2008 / Accepted: 2 March 2009 / Published online: 24 March 2009  
© Springer-Verlag 2009

**Abstract** Irrigation of olive orchards is challenged to optimize both yields and oil quality. Best management practices for olive irrigation will likely depend on the ability to maintain mild to moderate levels of water stress during at least some parts of the growing season. We examined a number of soil, plant and remote sensing parameters for evaluating water stress in bearing olive (var. Barnea) trees in Israel. The trees were irrigated with five water application treatments (30, 50, 75, 100 and 125% of potential evapotranspiration) and the measurements of soil water content and potential, mid-day stem water potential, and stomatal resistance were taken. Remote thermal images of individual trees were used to alternatively measure average canopy temperature and to calculate the tree's crop water stress index (CWSI), testing empirical and analytical

approaches. A strong non-linear response showing similar trends and behavior was evident in soil and plant water status measurements as well as in the CWSI, with decreasing rates of change at the higher irrigation application levels. No statistically significant difference was found between the analytical and the empirical CWSI, suggesting that the relative simplicity of the analytical method would make it preferable in practical applications.

## Introduction

The growing recognition of the health qualities of olive oil has led to an increase in its global consumption, which has almost doubled from the late 1990s to the early 2000s. Among other strategies, introduction and expansion of irrigation have served to fulfill the increased demand (Moriana et al. 2003). Irrigation has been shown to significantly increase tree- and orchard-scale oil yield (Gómez-Rico et al. 2006; Moriana et al. 2003; Patumi et al. 1999, 2002). However, studies have also indicated a tendency for irrigated olive trees to produce lower amounts of polyphenols (Berenguer et al. 2006; D'Andria et al. 1996; Dag et al. 2008; Gómez-Rico et al. 2007; Moriana et al. 2007; Patumi et al. 1999, 2002; Tovar et al. 2002a) and, in some cultivars, higher free fatty acid content (Dag et al. 2008). Likely, water stress is required to promote polyphenol production and high-quality oil (Berenguer et al. 2006; Patumi et al. 1999; Tovar et al. 2002b).

Water management where slight to moderate stress is maintained or where trees are submitted to stress conditions at specific phenological stages is expected to enable optimization of high yields with high-quality oil in olive orchards. In order to achieve this, crop water status must be

---

Communicated by S. Raine.

---

A. Ben-Gal · N. Agam · U. Yermiyahu · E. Presnov  
Institute of Soil Water and Environmental Sciences,  
Agricultural Research Organization,  
Gilat Research Center, 85280 M.P. Negev 2, Israel

V. Alchanatis · Y. Cohen · M. Sprintsin  
Institute of Agricultural Engineering,  
Agricultural Research Organization,  
The Volcani Center, Bet Dagan, Israel

I. Zipori · A. Dag  
Institute of Plant Sciences,  
Agricultural Research Organization,  
Gilat Research Center, 85280 M.P. Negev 2, Israel

A. Ben-Gal (✉)  
Environmental Physics and Irrigation,  
Agricultural Research Organization,  
Gilat Research Center, 85280 M.P. Negev 2, Israel  
e-mail: bengal@agri.gov.il

measured accurately and reliably with the aim of providing a pre-determined level of stress. In this study, the potential use of several measurement methods to monitor water status in olive orchards has been examined.

Crop water status may be determined by soil-based measurements, direct sensing of plant water status parameters, or indirect sensing of plant response to stress. Soil-based assessments include point measurements of water content and/or water potential and are limited due to the difficulty and expense of satisfactorily representing the heterogenic conditions found in the root zone (Campbell and Campbell 1982; Charlesworth 2005). Plant water stress may be measured as stem water potential, stomatal conductance, via sap-flow or as changes in leaf, stem or trunk size. All of the methods can accurately report actual crop water stress but their commercial relevance for monitoring water stress is limited due to sensitivity to other factors, spatial limitations and the difficulty of acquiring sufficient numbers of measurements for reliable representation of whole plants or fields (Jones 2004; Naor 2006). Accurate up-scaling of tree-based measurements to orchard scale, which is required for precise water stress management, is impractical. Methods that provide spatial measurements of indirect parameters associated with water stress are therefore advantageous.

Indirect measurements of water stress in plants are often based on leaf temperature, which is inversely correlated with transpiration and stomatal opening (Fuchs 1990). Canopy temperature has been used as an indicator for crop water stress since the 1960s. The ‘crop water stress index’ (CWSI) is based on the difference between canopy temperature, usually measured by infrared thermometry (IRT), and that of a ‘non-water stress baseline’ referring to the temperature of a well-watered crop (Jackson et al. 1981, 1988). Despite robust results with the CWSI approach for arid and semi-arid regions, limitations of its use as a routine tool stem from its high sensitivity to climate factors such as radiation, wind speed, and humidity, and from the need to establish crop-specific non-water-stressed baselines for different agroclimate zones (Jackson et al. 1988). Normalized CWSI using thermal imagery for canopy temperature measurements, combined with visible and near infrared images for exclusion of non-leaf material in temperature estimates, and natural or artificial wet and dry reference surfaces have been developed and used, and issues of their uniformity and reproducibility have been addressed (Fuchs 1990; Jones 2004; Meron et al. 2003). These techniques have been demonstrated to successfully measure water stress in cotton (Cohen et al. 2005; Sela et al. 2007) and in grapevines (Möller et al. 2007).

Sepulcre-Canto et al. (2006, 2007) used airborne hyperspectral (AHS) scanning imagery to differentiate water deficits and found partial correlation with ground-

based measurements on ‘Arbequina’ olive trees in Spain where higher temperatures were found for deficit compared to well-irrigated trees. The authors suggested that high-spatial thermal AHS imagery is capable of detecting water stress at the tree level as a function of canopy temperature.

In the present study the potential of using thermal images for in-field estimation of soil and crop water status of olive (cv. Barnea) under five different irrigation regimes was investigated. The specific aim was to compare thermal-based CWSI estimates with soil and plant water status parameters in order to evaluate the potential of CWSI for routine spatio-temporal monitoring of water status in olive orchards.

### Theory: the CWSI

Canopy temperature is indicative of water status in the leaves; however, it is influenced by other environmental conditions, mainly radiative flux, air temperature, wind speed, and relative humidity. In order to be applicable to varying conditions, canopy temperature, derived from a thermal image, must be normalized relative to a reference. The CWSI defines upper and lower boundary temperatures,  $T_{dry}$  and  $T_{wet}$ , representing a non-transpiring leaf and a fully transpiring leaf, respectively (Jones 1992):

$$CWSI = \frac{T_{canopy} - T_{wet}}{T_{dry} - T_{wet}} \quad (1)$$

with  $T_{canopy}$  the canopy temperature. The CWSI ranges from 0 to 1, indicating well-watered and stressed conditions, respectively.  $T_{dry}$  and  $T_{wet}$  can be derived either empirically or analytically.

### CWSI empirical ( $CSWI_E$ )

In the empirical approach,  $T_{dry}$  is set to 5°C greater than air temperature (Irmak et al. 2000) and  $T_{wet}$  is determined based on reference measurements of artificial wet cloth (Meron et al. 2003), with a typical size of 30 × 40 cm. Two main drawbacks limit the applicability of the CWSI for high spatio-temporal monitoring of stress. The first is the somewhat arbitrary value of 5°C. While it had indeed been proven to represent the maximum leaf temperature under several conditions (Cohen et al. 2005; Irmak et al. 2000; Möller et al. 2007), the CWSI is quite sensitive to the value assigned to  $T_{dry}$ , and a significant uncertainty is induced to the index’s value. The second drawback lies in the need for a wet reference to exist in every analyzed image. This limits the frequency at which data can be acquired, as well as determines a required high-spatial resolution (to detect a significant number of pixels within

the reference, while avoiding mixed pixels), thus limiting the usefulness of the method for routine measurements.

#### CWSI analytical (CSWI<sub>A</sub>)

To overcome the drawbacks of the empirical method, analytical expressions have been developed to compute  $T_{\text{dry}}$  and  $T_{\text{wet}}$ , based on the canopy energy balance (Jones 1999). The available energy at the canopy (i.e., the net radiation) is the sum of incoming and outgoing radiation ( $R_n$ ,  $\text{W m}^{-2}$ ):

$$R_n = R_{\text{SW}}(1 - \alpha) + R_{\text{LW}} \downarrow - R_{\text{LW}} \uparrow \quad (2)$$

$R_{\text{SW}}$  is the incoming short-wave radiation ( $\text{W m}^{-2}$ ),  $\alpha$  is the canopy albedo, and  $R_{\text{LW}} \downarrow$  and  $R_{\text{LW}} \uparrow$  are incoming and omitted long-wave radiations ( $\text{W m}^{-2}$ ), respectively:

$$R_{\text{LW}} \downarrow = 1.24 \left( \frac{0.1 e_{\text{air}}}{T_{\text{air}}} \right)^{1/7} \sigma T_{\text{air}}^4 \quad (3)$$

$$R_{\text{LW}} \uparrow = \varepsilon_{\text{canopy}} \sigma T_{\text{canopy}}^4$$

$e_{\text{air}}$  is the ambient water vapor pressure (kPa),  $T_{\text{air}}$  is the air temperature (K),  $\sigma$  is the Stephan–Boltzmann constant ( $= 5.67 \times 10^8 \text{ W m}^{-2} \text{ K}^{-4}$ ),  $\varepsilon_{\text{canopy}}$  is the canopy emissivity, and  $T_{\text{canopy}}$  is the canopy temperature (K). Neglecting the heat absorbed by the canopy,  $R_n$  is dissipated into sensible ( $H$ ,  $\text{W m}^{-2}$ ) and latent ( $\lambda E$ ,  $\text{W m}^{-2}$ ) heat fluxes, such that the energy balance of canopy is

$$R_n = H + \lambda E \quad (4)$$

Often, the canopy temperature in Eq. 3 is replaced by the air temperature and the isothermal net radiation  $R_{\text{ni}}$  is computed (Guilioni et al. 2008). The fact that the surface is not usually at air temperature is taken into account in a combined resistance to sensible heat transport ( $r_{\text{HR}}$ ,  $\text{s m}^{-1}$ ):

$$r_{\text{HR}} = \frac{1}{(1/r_{\text{H}}) + (1/r_{\text{R}})} \quad (5)$$

where  $r_{\text{H}}$  and  $r_{\text{R}}$  are the aerodynamic resistance to sensible heat transport and the resistance for radiative heat loss, respectively, both in ( $\text{s m}^{-1}$ ), parameterized by Jones (1992, 1999):

$$r_{\text{H}} = 100 \sqrt{\frac{d}{u}} \quad (6)$$

$$r_{\text{R}} = \frac{\rho C_p}{4\varepsilon\sigma T_{\text{air}}^3} \quad (7)$$

in which,  $d$  is the characteristic length of the leaves in the direction of the prevailing wind (m),  $u$  is the wind speed ( $\text{m s}^{-1}$ ),  $\rho$  is the dry air density ( $\text{kg m}^{-3}$ ),  $C_p$  is the specific heat of dry air at constant pressure ( $\text{J K kg}^{-1}$ ).

The sensible and latent heat fluxes are formulated as (Monteith and Unsworth 2008):

$$H = \frac{\rho C_p}{r_{\text{HR}}} (T_{\text{air}} - T_{\text{canopy}}) \quad (8)$$

and

$$\lambda E = \frac{\Delta r_{\text{HR}} R_{\text{ni}} + \rho C_p \text{VPD}}{\Delta r_{\text{HR}} + \gamma(r_{\text{V}} + r_{\text{S}})} \quad (9)$$

with VPD the vapor pressure deficit (kPa),  $\Delta$  the slope of saturated water vapor pressure versus temperature curve ( $\text{kPa } ^\circ\text{C}^{-1}$ ),  $\gamma$  the psychrometric constant ( $\approx 0.066 \text{ kPa K}^{-1}$ ),  $r_{\text{V}}$  the aerodynamic resistance to latent heat transport ( $\text{s m}^{-1}$ ), and  $r_{\text{S}}$  the stomatal resistance to sensible heat transport ( $\text{s m}^{-1}$ ). When the leaf does not transpire,  $\lambda E = 0$ , and all the available energies dissipate into sensible heat. Combining Eqs. 4 and 8, the upper boundary temperature ( $T_{\text{dry}}$ ) is

$$T_{\text{dry}} = T_{\text{air}} + \frac{R_{\text{ni}} r_{\text{HR}}}{\rho C_p} \quad (10)$$

When the leaf fully transpires,  $r_{\text{S}} \ll r_{\text{V}}$ , thus the stomatal resistance can be disregarded, and by rearranging Eqs. 4, 8, and 9, the lower boundary,  $T_{\text{wet}}$ , is computed:

$$T_{\text{wet}} = T_{\text{air}} - \frac{r_{\text{RH}} r_{\text{V}} \gamma}{\rho C_p (s r_{\text{HR}} + \gamma r_{\text{V}})} R_{\text{ni}} + \frac{r_{\text{HR}}}{s r_{\text{HR}} + \gamma r_{\text{V}}} \text{VPD} \quad (11)$$

The utilization of the analytical approach requires measurement of incoming solar radiation, air temperature, relative humidity, and wind speed. These measurements are available from any meteorological station, and can be representative for an entire field or orchard. Note that there is some uncertainty in the estimation of the resistances, which induces a level of uncertainty to this approach as well.

## Materials and methods

### Site description

The experiment was conducted in a 2 ha section of an 80 ha commercial orchard near Kibutz Kfar Menachem, Israel ( $31^\circ 44' \text{N}$ ,  $34^\circ 51' \text{E}$ ). Barnea var. trees spaced  $7 \times 4.25 \text{ m}$  were planted in 2001 and irrigated along with the surrounding commercial orchard until spring of 2006 when treatments began. In the year the measurements were conducted, 2007, the orchard was in an ‘on’ year with each tree carrying between 50 and 100 kg of fruit. The orchard was irrigated with secondary treated municipal effluent originating from the city of Jerusalem. The experimental section was divided into complete

random plots consisting of two central trees surrounded by trees receiving the same treatment. The two central trees in each plot were used for measuring water stress parameters with the other trees serving as a boundary. For each irrigation level, there were five replicate plots, such that ten trees per treatment could be measured. Irrigation was applied via individual delivery systems (mains, submains, laterals) for each treatment level. Each treatment had its own automation including valves, water meter and fertilizer meter. The orchard was irrigated via Uniram (Netafim, Israel) integral pressure compensated drippers ( $3.2 \text{ L h}^{-1}$ ) every 0.5 m in 20 mm diameter laterals. Fertilizer was given throughout the season at rates so that all treatments received  $220 \text{ kg ha}^{-1}$  nitrogen and  $300 \text{ kg ha}^{-1}$  potassium annually.

#### Irrigation treatments

Five levels of irrigation were applied. The irrigation application for each treatment was determined as a fraction of the daylight-hour potential evapotranspiration ( $ET_p$ ) calculated using Penman–Monteith equation (Monteith 1965). Meteorological data were collected from a station located adjacent to the orchard. Irrigation levels ranged from non-stressed (125 and 100%) to stress conditions (50 and 30%) through an intermediate level (75%). Actual daily irrigation ( $I$ ) was computed by

$$I = ET_p f_c \frac{\text{Irrlev}}{100} \quad (12)$$

where  $f_c$  is the cover factor estimated by mid-day shaded area and Irrlev is the level of irrigation for the different treatments (%).

In the second half of August 2007, the cover factor for all treatments was 0.5,  $ET_p$  was  $7.5 \text{ mm day}^{-1}$  and irrigation events occurred every other day. Winter (2006–2007) rainfall at the site was 525 mm. Irrigation was applied from 12 April through 30 November. Annual amounts of irrigation and daily water applied to each treatment at the time of the tree water stress evaluation are presented in Table 1. Plant and soil water status measurements were taken on 23 August 2007 between 1130 and

1430 hours. Irrigation was scheduled for that day and was postponed until after the measurements were completed.

#### Soil and plant water status measurements

Soil water content was measured gravimetrically from samples taken below the drip lateral midway between two trees at 0–30, 30–60 and 60–90 cm depths. Soil water potential was measured continuously using tensiometers (Irriwise, Netafim, Tel Aviv, Israel) placed 10 cm adjacent to the drip laterals, 1 m from trees at 30, 60 and 90 cm depths in a single replicate of each treatment. Depth-weighted averages for each replicate section were used as representative values for soil water content and potential. Stem water potential was assessed using a Scholander-type pressure chamber (Arimad, M.R.C., Holon, Israel) according to Gucci et al. (1997) on single west-facing shoulder height stems with five to seven new growth leaves that had been covered prior to 0700 hours on the day of measurements. Stomatal resistance was measured with a diffusion leaf porometer (SC-1, Decagon Devices Inc., Pullman, WA) on five leaves fully exposed to sunlight at shoulder level on each tree. Soil water content, soil water potential, stem water potential, and stomatal resistance measurements were all conducted simultaneously with the image acquisition.

#### Image acquisition and processing

Thermal images of the tree crowns were taken of six to eight individual trees of each irrigation level between 1130 and 1430 hours on 23 August 2007 with an uncooled infrared thermal camera. The camera (ThermaCAM model SC2000, FLIR Systems) has a  $320 \times 240$  pixel microbolometer sensor, sensitive in the spectral range of 7.5–13  $\mu\text{m}$ , and a lens with an angular field of view of  $24^\circ$ . Digital color (RGB) images were acquired with a digital camera (DSCF717, Sony Inc.) attached to the thermal camera. The two cameras were mounted on a truck-crane about 15 m above the canopy. The canopy height was about 4 m, so that the linear field of view at the canopy level was  $6 \times 6 \text{ m}$ , with spatial resolution of 2 cm. This resolution enabled discrimination between leaves and soil and selection of pixels that contained sunlit leaves. Aluminum crosses were placed in the camera's field of view in order to co-register the digital RGB and the thermal images. A wet artificial reference surface (WARS) was also placed in the camera's field of view. The WARS was constructed following Meron et al. (2003), as detailed by Cohen et al. (2005), to be a permanently wet surface of reproducible radiometric and physical properties.

Thermal images were processed with digital image processing tools using ThermaCamExplorer software

**Table 1** Annual (2007) and mean daily (23 August 2007) water quantities applied for each irrigation treatment level (Irrlev)

Irrlev (%)	Annual (mm)	Daily (mm)
30	201.6	1.1
50	332.5	1.9
75	498.5	2.8
100	663.2	3.8
125	818.1	4.7

(FLIR Systems, Sweden), Adobe Photoshop 7.0 software (Adobe Inc.) and Matlab R13 software (The Mathworks Inc., Natick, MA, USA). The raw thermal images were obtained in the FLIR Systems' proprietary format and converted to gray-scale images as described by Cohen et al. (2005). The centers of the aluminum crosses were selected as geographical control points and the thermal and RGB images were aligned and co-registered. The color image was used to select sunlit canopy pixels to produce a binary image where pixels belonging to the selected fraction are represented by logical 'one' and all other pixels are represented by logical 'zero'.

### Meteorological measurements

Global radiation, wind speed, air temperature and relative humidity were measured 1 m above the canopy by a meteorological station positioned within the experimental plot. The sampling rate was 0.1 Hz, and 1-min averages were recorded by a data acquisition system (CR10X, Campbell Scientific, Logan, UT, USA).

## Results and discussion

### Potential of the remotely sensed CWSI

The response of the olive trees to irrigation treatments, as detected by the various methods, is presented by the average value for each treatment (Fig. 1). Here, averages were chosen to minimize the effect of natural heterogeneity of the plants and to focus on the response to irrigation treatment. A strong non-linear response showing similar trends and behavior was evident in each method. Large responses were observed as irrigation was increased from low amounts (Irrlev = 30 and 50%) but smaller marginal responses were observed at higher irrigation applications. This demonstrates the response of the soil–plant–environment continuum as a whole. Soil water content and potential as well as stem water potential and stomatal resistance (Fig. 1a, b) showed high correlation coefficients ( $R^2$  ranging from 0.78 to 0.94) to irrigation amounts. It is noteworthy that decreased stomatal conductance in olive trees as a response to decreasing available water has previously been reported (e.g., Diaz-Espejo et al. 2007; Moriana et al. 2002), and the results presented here agree well with those studies. The remotely sensed indicators of plant water status (i.e., the canopy temperature and the empirical and analytical CWSI), which have not previously been tested for olives, showed a similar response to the irrigation treatments (Fig. 1c). Canopy temperature is a result of not only the plant's water status but also of the soil–biosphere–atmosphere interactions. Up to a certain

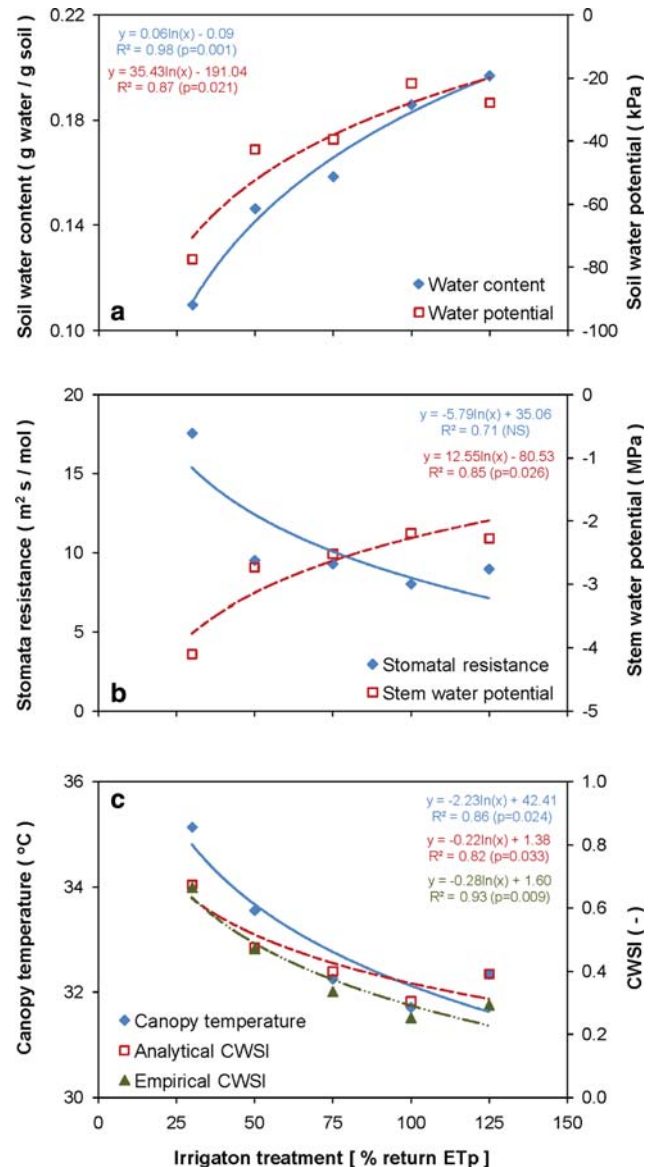


**Fig. 1** Water status detected by various methods as a response to irrigation treatments. Methods presented are soil water content and potential (a), stomatal resistance and stem water potential (b), and canopy temperature as well as analytical and empirical crop water stress index (CWSI) (c). Data points represent averages of all replicates for each irrigation treatment

threshold, an increase in leaf temperature (mainly due to exposure to high incoming short-wave radiation flux) enhances the photosynthetic activity. Under soil water stress conditions, stomatal closure further increases leaf temperatures beyond optimum values (Diaz-Espejo et al. 2007).

Since irrigation treatments are expected to alter transpiration flux, they are anticipated to cause corresponding canopy temperatures. By normalizing the canopy temperature (relative to high and low reference temperatures), the effect of environmental conditions is minimized and the water status is the main factor determining the index value.

In this study, both the empirical and the analytical indices showed a trend similar to that of the canopy temperature. This may be due to the short period of measurements, during which little change in the environmental conditions were observed. All three remote sensing-based techniques agreed well with the soil- and plant-based measures of water status, showing a clear response to varying irrigation levels.

The first step towards applying the remotely sensed CWSI as a routine management tool should be the establishment of its correlation with accepted and commonly used methods for estimating crop water stress. It is expected that the natural variability between the trees will be reflected by all methods. Data reported here show significant correlations of soil water potential and stomatal resistance versus the temperature and CWSI indices (Fig. 2). Soil water content seems to be less well correlated to the remote sensing methods. It is important to note that this analysis is performed on data acquired during  $\sim 4$  h of a single day, during which little variation in the environmental conditions were observed (see Fig. 4 and accompanying

discussion). The similar results obtained by the raw canopy temperature and the normalized indices are explained by this small variability. It is likely that multi-day datasets would show lower correlations with canopy temperature due to varying environmental conditions. The CWSI shows promise in replacing the traditional and laborious methods for estimating water status and level of stress in olive orchards (Fig. 2). In spite of this, the level of variation between the remote temperature measurements for individual treatments was larger than that of the plant-based measurements, indicating that the method for analyzing the thermal images and choosing pixels with sunlit leaves could be improved.

To study the relationships between the canopy temperature and the CWSIs and to determine a preferable method, the indices were regressed against the canopy temperature and each other (Fig. 3). The coefficient of determination ( $R^2$ ) between the  $CWSI_A$  and  $T_C$  was 0.89, and 0.80 for  $CWSI_E$  and  $T_C$ , indicating that for this 1 day measurement set the normalization process had little added value compared to the raw canopy temperature. This means that if the

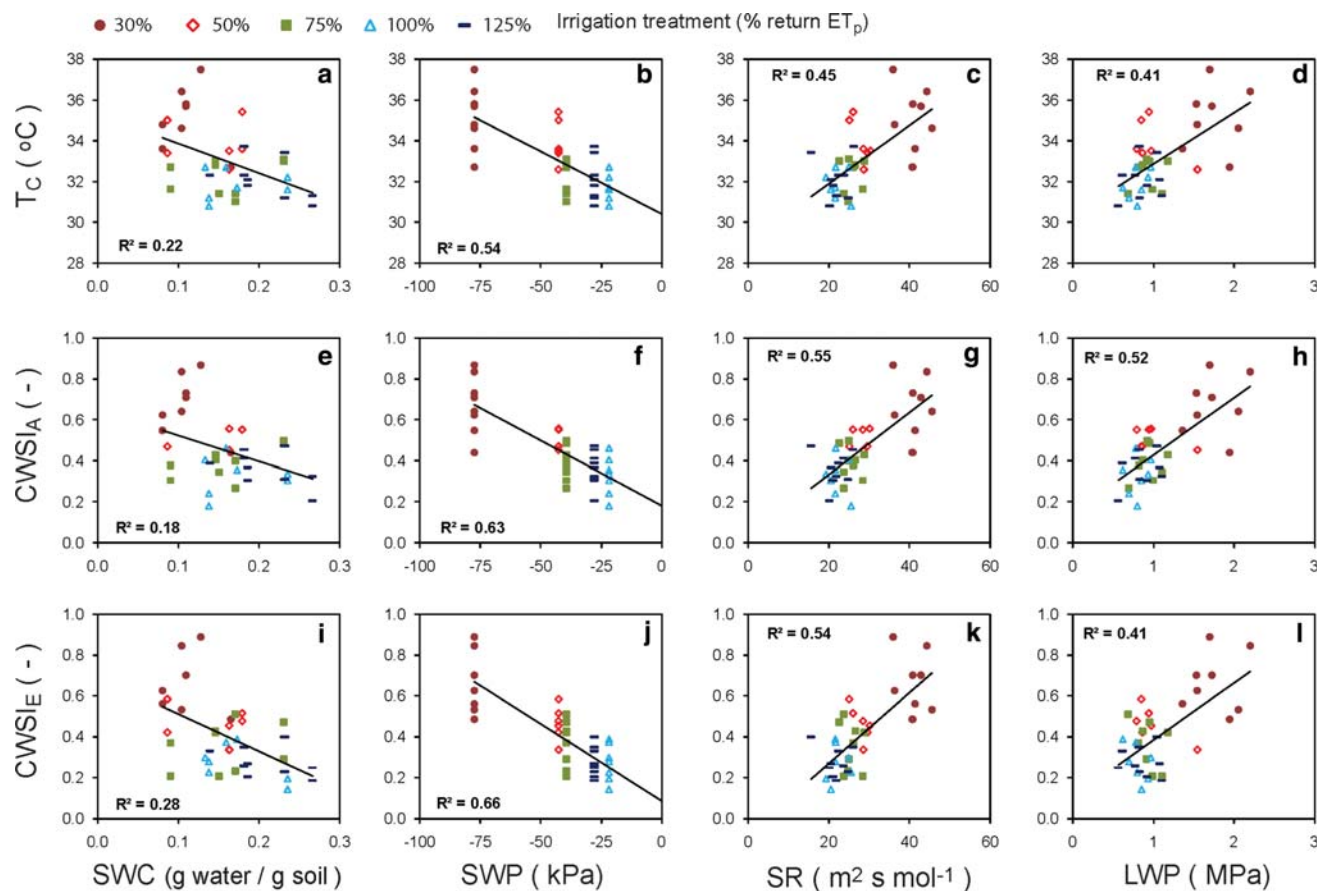
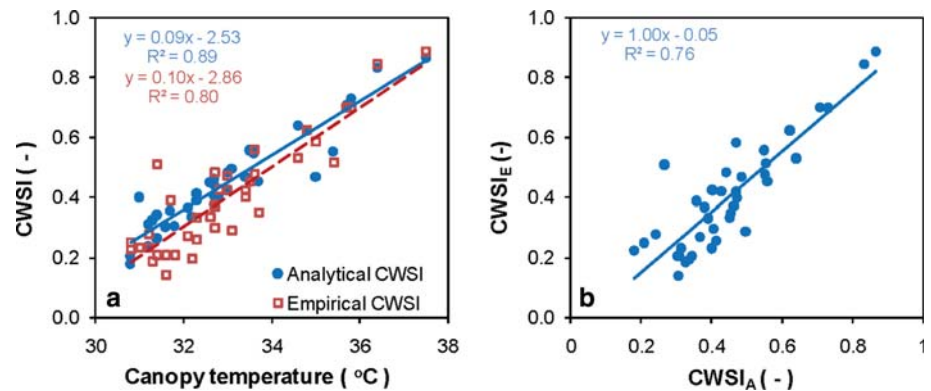


**Fig. 2** Correlations between the four “traditional” methods for evaluating water status: soil water content (SWC), soil water potential (SWP), stomatal resistance (SR), and stem water potential (SWP) and the proposed remote sensing-based methods: canopy temperature

( $T_C$ ), the analytical crop water stress index ( $CWSI_A$ ), and the empirical crop water stress index ( $CWSI_E$ ). Data points represent individual measurements. All regressions are highly significant ( $P < 0.01$ )

**Fig. 3** Crop water stress indices (CWSI) plotted versus canopy temperature (a) and versus themselves (b)



aim is to simply compare between water status of plants within a given plot at a given time, the canopy temperature may be a good indicator. However, if a comparison over time as plants develop is required, the removal of the influence of environmental conditions through the use of the normalized CSWI will likely be preferable to the canopy temperature alone.

Linear regression analysis between the two indices (Fig. 3b) produced a best fit line with a slope of 1.00 (not significantly different to 1) and an intercept of  $-0.05$  (not significantly different to 0), meaning that the analytical and the empirical CWSIs yielded similar results. Similar results were found by Gontia and Tiwari (2008) for a wheat crop. The analytical index does not require a wet reference, thus its application is simpler, and has more potential to be widely applied. Therefore, based on this dataset,  $CWSI_A$  appears to be preferable. Further research will need to be conducted to assess this finding over a larger range of environmental conditions. Nevertheless, both methods agreed well with the traditional methods of determining crop water status and show promising potential for routine monitoring of water status at the orchard scale.

#### Time of thermal image acquisition

One of the advantages of the remote sensing method is that a snapshot of both thermal and RGB images can be taken instantaneously to provide simultaneous information regarding large parts of the orchard. Where the images are taken only once a day, the optimal time of image acquisition to detect crop stress needs to be determined.

The main driving forces of  $ET_p$  (i.e., incoming short-wave radiation, air temperature, relative humidity, and wind speed) showed some changes over the duration of data collection (Fig. 4). In particular, the incoming radiation increased until 1300 hours (local time) and decreased thereafter, and the relative humidity had a general increasing trend with a decrease at the beginning of the study period and between 1300 and 1400 hours. An increasing level of measured stress (in terms of  $T_{\text{canopy}} - T_{\text{air}}$ ) is also apparent

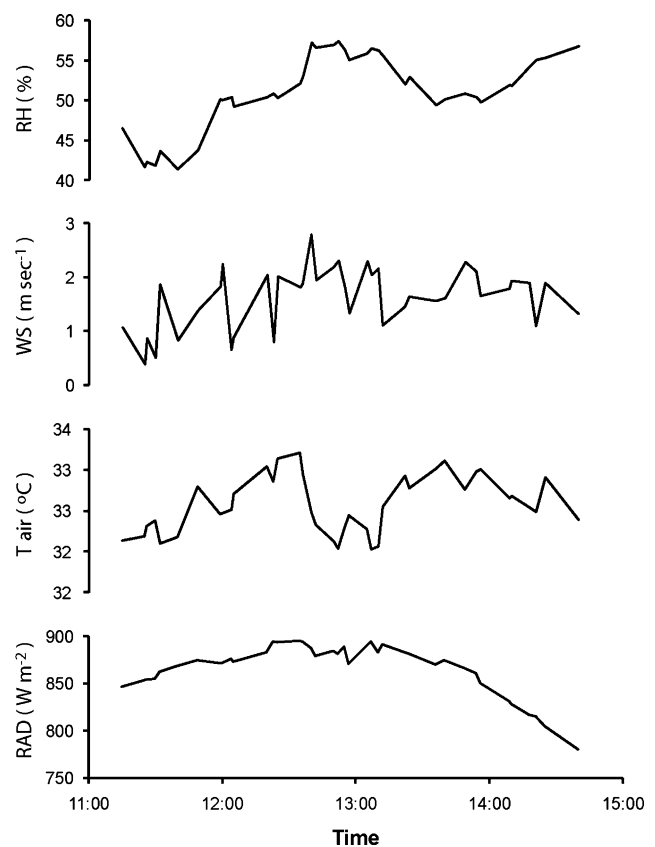


**Fig. 4** Prime environmental conditions ( $RAD$  incoming short-wave radiation,  $T_{\text{air}}$  air temperature,  $WS$  wind speed,  $RH$  relative humidity) throughout the experiment period on 23 August 2007

(Fig. 5). It is expected that the temperature of transpiring leaves will be at or lower than air temperature, and that the temperature of stressed leaves will be higher than air temperature (Diaz-Espejo et al. 2007). Indeed, the canopy temperatures of the trees were stratified according to the irrigation treatments (Fig. 5). The canopy temperature of the stressed trees ( $Irrlev = 30$  and  $50\%$ ) was above air temperature for all trees except those sampled at the beginning of the experiment, while canopy temperature of the well-watered trees ( $Irrlev = 100$  and  $125\%$ ) remained below air

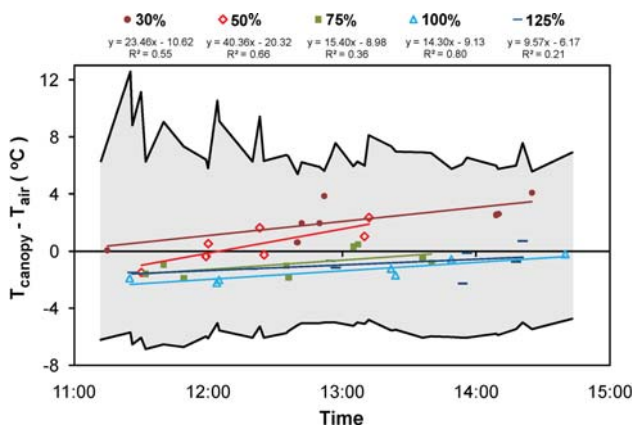


**Fig. 5** Temperature deviations from air temperature: the *upper* and *lower* black lines are the boundary canopy temperatures ( $T_{dry}$  and  $T_{wet}$ ); the *shaded area* between the two boundary lines represents the range within which canopy temperature ( $T_{canopy}$ ) is expected to fall; and the *colored circles* are the deviations of canopy temperature from air temperature ( $T_{air}$ ) of the various irrigation treatments. Note that only regressions of treatments 25 and 125% are significant. See text for more details

temperature, excluding one tree sampled towards the end of the experiment which had a temperature slightly higher than air temperature. The Irrlev = 75% treatment had values in between these two groups.

An increase in  $\Delta T$  with time was apparent for all treatments, with a corresponding increase in the CWSI values (Fig. 6). Since both  $CWSI_A$  and  $CWSI_E$  behaved similarly, data are shown for  $CWSI_A$  only. At the beginning of the experiment, trees of all treatments had a lower CWSI compared to trees of the same treatment sampled later, with a larger increase in CWSI for the stressed treatments. This implies that at the beginning of the experiment, the stomata of all trees were open to some extent, thus differences in canopy temperatures induced by the irrigation treatments

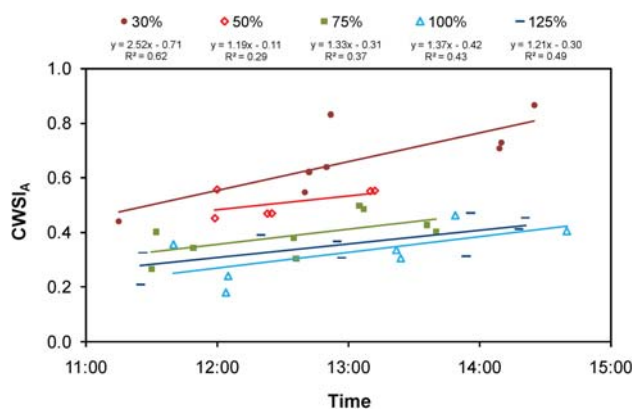


**Fig. 6** Change in crop water stress index (CWSI) with time. The *different symbols and colors* represent the various irrigation treatments. Note that only regressions of treatments 25 and 125% are significant. See text for more details

were relatively small. Towards noon and early afternoon, stomata of the stressed trees started closing after transpiring and losing water, resulting in an increase in canopy temperature. Note that while only the trends of the 30 and 125% treatments were statistically significant (Figs. 5, 6), regressions of the combined data of the stressed treatments (30 and 50%) and the well-watered treatments (100 and 125%) were both highly significant, indicating that the small number of replicates is the likely reason for the non-significant regression lines. Similar findings were reported by Moriana et al. (2002) where in all irrigation treatments stomatal conductance was highest in the morning and declined continuously towards the afternoon, and water availability had a significant effect on the rate of decrease.

Interestingly, Sepulcre-Canto et al. (2006, 2007) observed a better relationship between  $\Delta T$  and stomatal resistance early in the morning and a deterioration in the relationship towards noon. Their explanation of these findings was that during the early morning hours the soil temperature is lower, and thus has a smaller influence on the measurements. The major difference between their assessment of the CWSI to the approach presented here is that Sepulcre-Canto et al. (2006, 2007) did not mask the soil and used the original mixed pixels in their assessments of temperature. In such an approach, the contribution of the soil is expected to increase towards noon, and may interfere with the canopy signal. Since the soil is masked out in the approach used here, it does not affect the signal or affect the CWSI computation. Therefore, in this case, the stronger the stress, the larger the CWSI value, leading to a better assessment of water status in the trees.

While similar diurnal trends for stem water potential and stomatal resistance measurements were anticipated, these were not detected. This may be because the variability between individual trees was larger than the response of each tree to the development of stress during the day. It is hypothesized that if measurements of individual trees were repeated several times during this period, similar trends would have been revealed. Unfortunately, the data collected for this study cannot assess this hypothesis.

If only one snapshot is to be taken, the time at which differences between treatments are best detected is the time of maximum stress. This means that, within the timeframe examined in this study, the best time for image acquisition is early afternoon. Future study is planned for a closer examination of the diurnal dynamics in order to determine the optimum time at which CWSI is best applied.

## Summary and conclusions

The understanding that water stress can contribute to optimization of olive oil yield and quality has inspired

investigation of water management strategies where slight to moderate stress is maintained or where olive trees are submitted to stress conditions at specific phenological stages. Commercially, such water management will be possible only by the development of a method for routine estimates of orchard-scale water status. The specific aim of this study was to compare thermal-based CWSI estimates that can potentially provide routine measurements, with more traditional soil and plant water status parameters.

Both the empirical and the analytical CWSI were highly correlated with the soil and plant water status methods, showing promise for routine monitoring of water status for olives at the orchard scale. As both indices yielded similar results, and given the relative practicality of the analytical index, it appears that the analytical CWSI has an advantage over the empirical CWSI. Further research is required to assess this finding over a larger range of environmental conditions.

As for determining the best time of image acquisition, it is clear that the time at which differences between treatments are best detected is the time of maximum stress. This means that the best time for image acquisition is early afternoon. Future study is planned for a closer examination of the diurnal dynamics in order to determine the optimum time at which CWSI is best applied.

**Acknowledgments** This work was supported by The Chief Scientist of Israel's Ministry of Agriculture and Rural Development (award #304-0300), the Middle East Regional Irrigation Management Information System (MERIMIS/USDA-ARS), and the Netafim Company. Special thanks to TZABA"R KA"MA for technical and horticultural support and cooperation in establishing and maintaining the experimental orchard.

## References

- Berenguer MJ, Vossen PM, Grattan SR, Connell JH, Polito VS (2006) Tree irrigation levels for optimum chemical and sensory properties of olive oil. *HortScience* 41:427–432
- Campbell GS, Campbell MD (1982) Irrigation scheduling using soil moisture measurements: theory and practice. *Adv Irrig* 1:25–42
- Charlesworth P (2005) Soil water monitoring. CSIRO/CRC irrigation futures. Land and Water Australia, Canberra
- Cohen Y, Alchanatis V, Meron M, Saranga Y, Tsipris J (2005) Estimation of leaf water potential by thermal imagery and spatial analysis. *J Exp Bot* 56(417):1843–1852
- D'Andria R, Morelli G, Martuccio G, Fontanazza G, Patumi M (1996) Evaluation of yield and oil quality of young olive trees under different irrigation regimes. *Italus Hortus* 3:23–31
- Dag A et al (2008) The effect of irrigation level and harvest mechanization on virgin olive oil quality in a traditional rain-fed "Souri" olive orchard converted to irrigation. *J Sci Food Agric* 88:1524–1528
- Diaz-Espejo A, Nicolas E, Fernandez JE (2007) Seasonal evolution of diffusional limitations and photosynthetic capacity in olive under drought. *Plant Cell Environ* 30(8):922–933
- Fuchs M (1990) Infrared measurement of canopy temperature and detection of plant water-stress. *Theor Appl Climatol* 42(4):253–261
- Gómez-Rico A, Salvador MD, La Greca M, Fregapane G (2006) Phenolic and volatile compounds of extra virgin olive oil (*Olea europaea* L. Cv. Cornicabra) with regards to fruit ripening and irrigation management. *J Agric Food Chem* 54:7130–7136
- Gómez-Rico A et al (2007) Influence of different irrigation strategies in a traditional Cornicabra cv. olive orchard on virgin olive oil composition and quality. *Food Chem* 100:568–578
- Gontia NK, Tiwari KN (2008) Development of crop water stress index of wheat crop for scheduling irrigation using infrared thermometry. *Agric Water Manage* 95(10):1144–1152
- Gucci R, Lombardini L, Tattini M (1997) Analysis of leaf water relations in two olive (*Olea europaea*) cultivars differing in tolerance to salinity. *Tree Physiol* 17:13–21
- Guilioni L, Jones HG, Leinonen I, Lhomme JP (2008) On the relationships between stomatal resistance and leaf temperature in thermography. *Agric For Meteorol* 148:1908–1912
- Irmak S, Haman DZ, Bastug R (2000) Determination of crop water stress index for irrigation timing and yield estimation of corn. *Agron J* 92(6):1221–1227
- Jackson RD, Idso SB, Reginato RJ, Pinter JPJ (1981) Canopy temperature as a drought stress indicator. *Water Resour Res* 17:1133–1138
- Jackson RD, Kustas WP, Choudhury BJ (1988) A re-examination of the crop water stress index. *Irrig Sci* 9:309–317
- Jones HC (1992) Plants and microclimate. Cambridge University Press, Cambridge
- Jones HG (1999) Use of infrared thermometry for estimation of stomatal conductance as a possible aid to irrigation scheduling. *Agric For Meteorol* 95(3):139–149
- Jones HG (2004) Irrigation scheduling: advantages and pitfalls of plant-based methods. *J Exp Bot* 55:2427–2436
- Meron M, Tsipris J, Charitt D (2003) Remote mapping of crop water status to assess spatial variability of crop stress. In: Stafford J, Werner A (eds) Precision agriculture. Proceedings of the fourth European conference on precision agriculture. Academic Publishers, Berlin, pp 405–410
- Möller M et al (2007) Use of thermal and visible imagery for estimating crop water status of irrigated grapevine. *J Exp Bot* 58(4):827–838
- Monteith JL (1965) Evaporation and environment. *Symp Soc Exp Biol* XIX:205–234
- Monteith JM, Unsworth MH (2008) Principles of environmental physics. Elsevier, New York
- Moriana A, Villalobos FJ, Fereres E (2002) Stomatal and photosynthetic responses of olive (*Olea europaea* L.) leaves to water deficits. *Plant Cell Environ* 25(3):395–405
- Moriana A, Orgaz F, Fereres E, Pastor M (2003) Yield responses of a mature olive orchard to a water deficits. *J Am Soc Hortic Sci* 128:425–431
- Moriana A et al (2007) Irrigation scheduling for traditional, low-density olive orchards: water relations and influence on oil characteristics. *Agric Water Manag* 87:171–179
- Naor A (2006) Irrigation scheduling and evaluation of tree water status in deciduous orchards. *Hortic Rev* 32:111–165
- Patumi M et al (1999) Yield and oil quality of intensively trained trees of three cultivars of olive (*Olea europaea* L.) under different irrigation regimes. *J Hortic Sci Biotechnol* 74:729–737
- Patumi M et al (2002) Olive and olive oil quality after intensive monocone olive growing (*Olea europaea* L., cv. Kalamata) in different irrigation regimes. *Food Chem* 77:27–34
- Sela E et al (2007) Thermal imaging for estimating and mapping crop water stress in cotton. In: Stafford JV (ed) European conference

- in precision agriculture 2007. Wageningen Academic Publications, The Netherlands, pp 365–371
- Sepulcre-Canto G et al (2006) Detection of water stress in an olive orchard with thermal remote sensing imagery. *Agric For Meteorol* 136(1–2):31–44
- Sepulcre-Canto G et al (2007) Monitoring yield and fruit quality parameters in open-canopy tree crops under water stress. Implications for ASTER. *Remote Sens Environ* 107(3):455–470
- Tovar MJ, Romero MP, Alegria S, Girona J, Motilva MJ (2002a) Composition and organoleptic characteristics of oil from Arbequina olive (*Olea europaea* L) trees under deficit irrigation. *J Sci Food Agric* 82:1755–1763
- Tovar MJ, Romero MP, Girona J, Motilva MJ (2002b) L-Phenylalanine ammonia-lyase activity and concentration of phenolics in developing olive (*Olea europaea* L. cv Arbequina) fruit grown under different irrigation regimes. *J Sci Food Agric* 82:892–898